Moving Surface Boundary-Layer Control as Applied to Two-Dimensional Airfoils

V. J. Modi,* F. Mokhtarian,† and M. S. U. K. Fernando‡
The University of British Columbia, Vancouver, British Columbia, Canada
and
T. Yokomizo§
Kanto Gakuin University, Yokohama, Japan

The concept of moving surface boundary-layer control, as applied to a Joukowsky airfoil, is investigated through an experimental program complemented by a flow visualization study. The moving surface was provided by rotating cylinders located at the leading edge and upper surface of the airfoil. The results suggest that the leading-edge rotating cylinder effectively extends the lift curve without substantially affecting its slope, thus increasing the maximum lift and delaying stall. When used in conjunction with a second cylinder on the upper surface, further improvements in the maximum lift and stall angle are possible. The maximum coefficient of lift realized was around 2.73, approximately three times that of the base airfoil. The maximum delay in stall was around 48 deg. In general, the performance improves with an increase in the ratio of cylinder surface speed U_c to the freestream speed U. However, the additional benefit derived progressively diminishes with an increase in U_c/U and becomes virtually negligible for $U_c/U > 4$. There appears to be an optimum location for the cylinder at the upper side of the leading edge that gave quite promising results. Although the $C_{L,\max}$ obtained was a little lower than the two-cylinder configuration (2.35 against 2.73), it offers a major advantage in terms of mechanical simplicity.

Introduction

EVER since the introduction of the boundary-layer concept by Prandtl, there has been a constant challenge faced by scientists and engineers to minimize its adverse effects and control it to advantage. Methods such as suction, blowing, vortex generators, turbulence promoters, etc., have been investigated at length and employed in practice with a varying degree of success. A vast body of literature accumulated over the years has been reviewed rather effectively by several authors including Goldstein,[1] Lachmann,[2] Rosenhead,[3] Schlichting,[4] Chang,[5] and others. However, the use of moving wall for boundary-layer control has received relatively less attention. Modi et al.[6] have reviewed this literature at considerable length.

Irrespective of the method used, the main objective of a control procedure is to prevent or at least delay the separation of boundary layer from the wall. A moving surface attempts to accomplish this in two ways:

1) It retards the initial growth of the boundary layer by minimizing relative motion between the surface and the freestream.

2) It injects momentum into the existing boundary layer.

The most practical application of moving wall for boundary-layer control was demonstrated by Favre.[7] Using an airfoil with upper surface formed by a belt moving over two rollers, he was able to delay separation until the angle of attack reached 55 deg, where the maximum lift coefficient of 3.5 was realized. Alvarez-Calderon and Arnold[8] carried out tests on a rotating cylinder flap to evolve a high-lift airfoil for STOL-type aircraft. The system was flight tested on a single engine high-wing research aircraft designed by Aeronautics Division of the Universidad Nacional de Ingenieria in Lima, Peru.[9]

Of some interest is the North American Rockwell designed OV-10A aircraft, which was flight tested by the NASA Ames Research Center.[10-12] Cylinders, located at the leading edges of the flaps, are made to rotate at high speed with the flaps in lowered position. The main objective of the test program was to assess handling qualities of the propeller-powered STOL-type aircraft at higher lift coefficients. The aircraft was flown at speeds of 29–31 m/s along approaches up to −8 deg (i.e., glide path with respect to the horizontal), which corresponded to a lift coefficient of about 4.3. In the pilot's opinion, any further reductions in approach speed were limited by the lateral-directional stability and control characteristics.

So far as the effect of a rotating cylinder located at the nose and/or at the trailing edge of an airfoil is concerned the available literature is rather scarce and has been reviewed by Mokhtarian and Modi.[13] Their own wind-tunnel and numerical experiments with two-dimensional models of a Joukowsky airfoil led to several useful conclusions[13,14]:

1) The numerical surface singularity method, in conjunction with a relatively simple boundary-layer correction scheme, represents a promising approach for modeling the moving surface boundary-layer control. The predicted pressure distributions are in good agreement with the experiment almost up to the point of complete separation from the airfoil surface except near the trailing edge, where more accurate description of the flowfield would require representation of the separated flow region using a precise viscous-correction procedure.

2) The leading-edge rotating cylinder extends the lift curve without substantially affecting its slope, thus effectively increasing the maximum lift and delaying stall. In general, the performance improves with an increase in the ratio of cylinder surface speed U_c to the freestream speed U. However, the additional benefit derived progressively diminishes with an increase in U_c/U. With the cylinder rotation, the flow never separated completely from the upper surface for angles of attack as high as 49 deg. The higher rates of rotation

Presented as Paper 89-0296 at the AIAA 27th Aerospace Sciences Meeting, Reno, NV, Jan. 9–12, 1989; received April 15, 1989; revision received Jan. 29, 1990.

*Professor, Department of Mechanical Engineering. Fellow AIAA.
†Graduate Research Assistant, Department of Mechanical Engineering; presently Staff Engineer, Canadair Ltd., Montreal, Canada.
‡Post-Doctoral Fellow, Department of Mechanical Engineering.
§Professor, Department of Mechanical Engineering.

($U_c/U > 1$) promoted reattachment of the partially separated flow and increased the lift coefficient by as much as 150% for $U_c/U = 4$.

3) A rotating trailing-edge cylinder affects the airfoil characteristics in a fundamentally different manner. It acts as a flap and shifts the C_L vs α curves to the left, thus increasing the lift coefficients before stall. For example, at $\alpha = 4$ deg, it increased the C_L by about 320%. In conjunction with the leading-edge cylinder, it can provide significant improvements in lift over the entire range of small to moderately high angles of incidence ($\alpha \leq 18$ deg).

The investigation reported here builds upon this body of literature. It studies fluid dynamics of an airfoil with the moving surface boundary-layer control using an extensive wind-tunnel test program. With information concerning the effect of the leading- and trailing-edge cylinders on the boundary-layer control in hand, the focus is on the injection of momentum at various locations on the top surface of the airfoil. One would also like to know if there is an optimum location of the rotating cylinder(s) in terms of the $C_{L,\max}$, delay in stall, etc. The experimental study uses a multisection symmetrical Joukowsky model, which allows the use of one or more rotating cylinders at various locations around the airfoil.

Wind-Tunnel Test Program

The wind-tunnel model, a symmetrical Joukowsky airfoil of 15% maximum thickness to chord ratio, approximately 0.38 m along chord and 0.68 m long, spanned the tunnel test section, $0.91 \times 0.68 \times 2.6$ m, to create essentially two-dimensional conditions. The model was provided with pressure taps, suitably distributed over the circumference, to yield detailed information concerning the surface loading. It was supported by an Aerolab six-component strain gauge balance and tested in a low-speed, low-turbulence return-type wind tunnel where the airspeed can be varied from 1–50 m/s with a turbulence level of less than 0.1%. A Betz micromanometer with an accuracy of 0.2 mm of water was used to measure pressure differential across the contraction section of 7:1 ratio. The rectangular test section (0.91×0.68 m) is provided with 45 deg corner fillets that vary from 15.25×15.25 to 12×12 cm to partly compensate for the boundary-layer growth. The spatial variation of velocity in the test section is less than 0.25%.

To provide flexibility in locating the cylinder on the airfoil and permit testing of multicylinder configurations, a sectional design was adopted. The model consists of an aluminum skin wrapped around an aluminum and steel frame with various sections of the surface removable, as required, to accommodate cylinders. A schematic diagram of the model in Fig. 1 shows details of the construction, including the leading-edge rotating cylinder. A nose fill-in section replaced the leading-edge cylinder when it was not used as a rotating element. The top panel was removed to house the upper-surface cylinders at locations shown in Fig. 2.

The rotating cylinders were mounted between high-speed bearings housed in the brackets at either end of the model. They were driven by 1/4 hp, 3.8 A variable speed motors, located outside the tunnel, through standard couplings.

The configurations tested include the leading-edge cylinder, the forward upper-surface cylinder, the rear upper-surface cylinder, the leading-edge and upper-surface cylinders, and the upper leading-edge cylinder.

The model was provided with a total of 44 pressure taps, distributed over the circumference, to yield detailed information about the surface loading. However, once a section of the model was removed to accommodate a cylinder, the pressure taps in that section were lost. Although the pressure information over the small region represented by the upper-surface cylinder is not of particular significance, the corresponding data at the leading edge of the airfoil is crucial since it represents a high-suction region. Its measurement presented a challenging task. Locating pressure taps on the surface of the cylinder, typically rotating in the range of 2000–7000 rpm offers considerable practical difficulty. The problem was resolved by measuring the pressure in the immediate vicinity of the cylinder rather than on the surface itself.

This was achieved in the case of the leading-edge cylinder by keeping the pressure taps stationary while the cylinder rotated. By locating the tap in a narrow ring, the width of

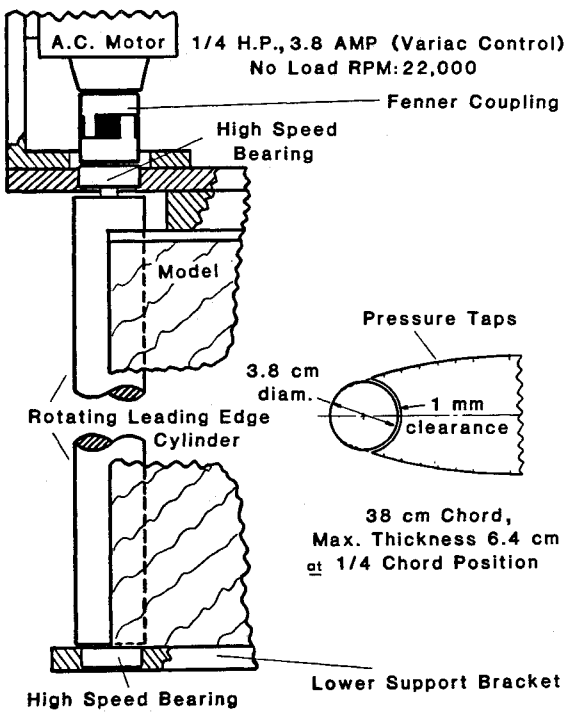

Fig. 1 Detailed schematic of the leading-edge rotating cylinder and cylinder-drive mechanism.

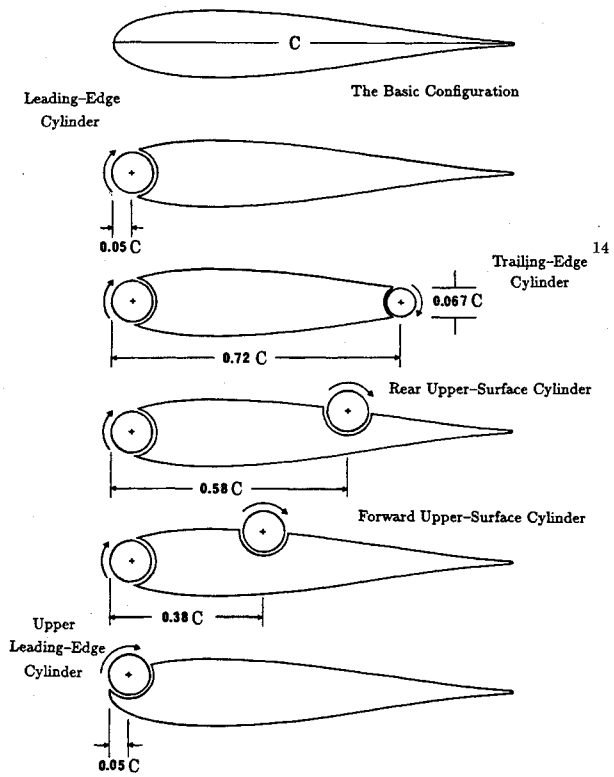

Fig. 2 Various rotating-cylinder configurations studied with the Joukowsky airfoil model.

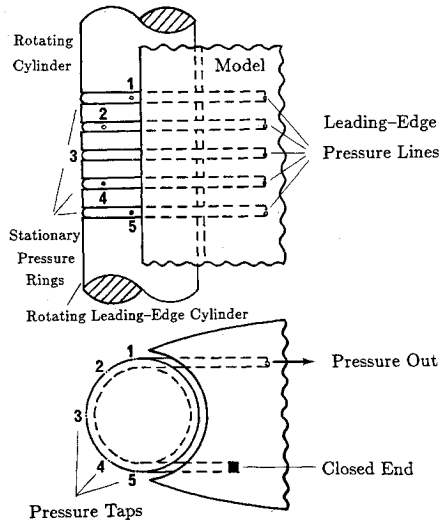

Fig. 3 Schematic diagram of the leading-edge construction of the Joukowsky model showing the details of the pressure taps.

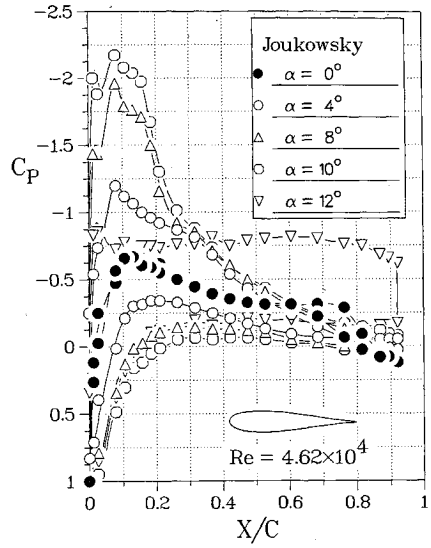

Fig. 4 Experimentally obtained pressure distributions for the basic Joukowsky model.

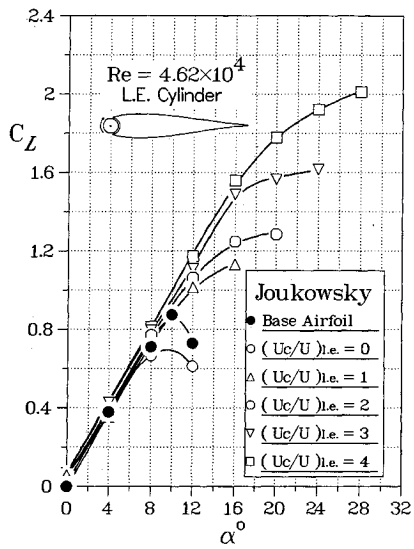

Fig. 5 Effect of the leading-edge cylinder rotation on the lift and stall characteristics of the Joukowsky model.

which represented only a very small fraction of that of the cylinder, it was possible to ensure the continuity of flow over the entire surface and to obtain an estimate of the surrounding pressure. The leading-edge cylinder was provided with grooves to house the "pressure rings" while maintaining the cylinder surface uniform. Figure 3 shows details of the leading-edge geometry and position of the pressure taps.

The tests were conducted over an extended range of angles of attack and cylinder rotational speeds, corresponding to $U_c/U = 0,1,2,3,4$, at a Reynolds number of 4.62×10^4. The choice of the Reynolds number in this case was dictated by vibration problems with multicylinder configurations operating at high rotational speeds (around 8000 rpm for $U_c/U = 4$). The pressure plots were integrated in each case to obtain the lift coefficient.

The lift was also measured independently using an Aerolab six-component strain gauge balance to assess two-dimensional character of the flow. To that end, the model was mounted with its spanwise axis perpendicular to the supporting platform of the balance and the wall clearance at either end of the model was kept to a minimum (less than 3 mm). The tests were carried out at several angles of attack and cylinder rotational speeds. The cylinder rotation introduced high-frequency modulations to the force signal, which were eliminated using a band-pass filter. The force data correlated remarkably well with the pressure integrated values. The difference between the two depended on α and U_c/U but was never more than 4%, the estimated error range of the measuring instrumentation.

Results and Discussion

The relatively large angles of attack used in the experiments result in a considerable blockage of the wind-tunnel test section, from 21% at $\alpha = 30$ deg to 30% at $\alpha = 45$ deg. The wall confinement leads to an increase in local wind speed at the location of the model, thus resulting in an increase in aerodynamic forces. Several approximate correction procedures have been reported in literature to account for this effect. However, these procedures are mostly applicable to streamlined bodies with attached flow. A satisfactory procedure applicable to a bluff body offering a large blockage in a flow with separating shear layers is still not available.

With rotation of the cylinder(s), the problem is further complicated. As shown by the pressure data and confirmed by the flow visualization, the unsteady flow can be separating and reattaching over a large portion of the top surface. In absence of any reliable procedure to account for wall confinement effects in the present situation, the results are purposely presented in the uncorrected form.

The pressure distribution data for the "base airfoil" (in absence of the modifications imposed by the leading-edge and upper-surface cylinders) are presented in Fig. 4. The leading edge was now formed by a snugly fitting plug (the nose fill-in section). Due to practical difficulty in locating pressure taps in the cusp region, there is an apparent discontinuity in the pressure plots near the trailing edge. However, this region has little importance in the present discussion. It is apparent that the airfoil, in absence of any modifications to its nose geometry, stalls at an angle of attack of around 10–12 deg. These results serve as reference to assess the effect of rotating cylinders in different locations.

Note that the wall confinement effect at $\alpha = 10$ deg is relatively small, as the blockage ratio is around 7%. More importantly, focus here is on the effect of the momentum injection due to the cylinder rotation with the aerofoil at a given angle of attack. Results of the flow visualization study, presented later, emphasize this point.

Figure 5 summarizes the effects of modification of the airfoil with the leading-edge cylinder and the cylinder rotation. The base airfoil has a maximum lift coefficient of about 0.87 at an angle of attack of 10 deg. There is a penalty associated with the modified nose geometry as well as due to the gap, but even at the lowest rate of rotation of the cylinder ($U_c/U = 1$) the lift and stall characteristics are significantly

improved. The airfoil exhibits a desirable flattening of the lift curve at stall. The maximum lift coefficient measured with $U_c/U = 4$ was around 2 at $\alpha = 28$ deg, which is almost three times the lift coefficient of the base airfoil.

Typical pressure plots at a relatively larger angle of attack are presented in Fig. 6 to assist in more careful examination of the local flowfield. As the angle of attack of the airfoil is increased, the flow starts to separate from the upper surface closer to the leading edge. At $\alpha = 16$ deg, for example, the cylinder rotating at $U_c/U = 1$ only keeps the flow attached at the leading edge. However, as the rate of rotation is increased, the size of the separated region is reduced, and at the higher rates of rotation the flow is again completely attached. Note that the point of separation on the upper surface clearly moves downstream with an increasing rate of rotation. The flow separates at around $X/C = 25\%$ with $U_c/U = 2$, around $X/C = 80\%$ when U_c/U is increased to three, and at the trailing edge with the highest U_c/U used. The flow visualization study discussed later substantiated this general behavior rather dramatically.

The forward and rear upper-surface cylinders, located at 38% and 58% chord, respectively, were considered independently and with either operating in conjunction with the leading-edge cylinder. As can be expected, in absence of rotation, their protrusion into the upper-surface flow had an adverse effect on the aerodynamic characteristics of the model. The flow separated at the location of the cylinder, resulting in a lower lift and increased drag. On the other hand, with rotation, either of the upper-surface cylinders was successful in attaining a higher $C_{L,\max}$ and delaying the stall (Fig. 7, $\alpha > 10$ deg). In this respect, the forward upper-surface cylinder was particularly effective.

Results of the trailing-edge cylinder from Ref. 14 are also included for comparison. It is apparent that the trailing-edge cylinder acts effectively as a flap, considerably increasing the lift at the smaller angles of attack ($\alpha < 8$ deg). It also leads to higher $C_{L,\max}$ compared to the upper-surface cylinders.

Typical pressure distribution data for the rear upper-surface cylinder in a combined configuration with the leading-edge cylinder are shown in Fig. 8 at medium to moderately high angles of attack. Contribution of the individual cylinder rotation is particularly noticeable at the lower rates of rotation. For example, $U_c/U = 1$ at $\alpha = 16$ deg (Fig. 8a) results in attached flow at the leading edge, primarily due to rotation of the leading-edge cylinder. The flow separates, however, further downstream (near $X/C \approx 0.1$) due to a large adverse pressure gradient. The rear upper-surface cylinder rotation causes the flow to reattach, but it separates again near the trailing edge. Increasing the cylinder rotation rate to

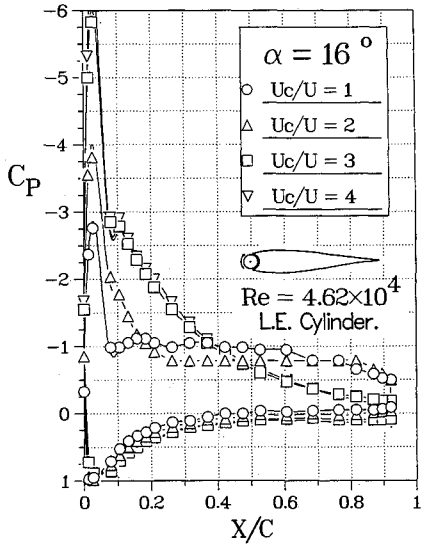

Fig. 6 Effect of increasing the rate of cylinder rotation on pressure distribution around the model at relatively larger angles of attack of $\alpha = 16$ deg.

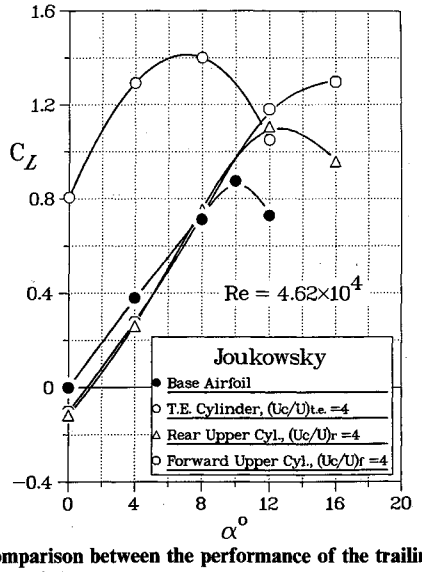

Fig. 7 A comparison between the performance of the trailing-edge and upper-surface cylinders.

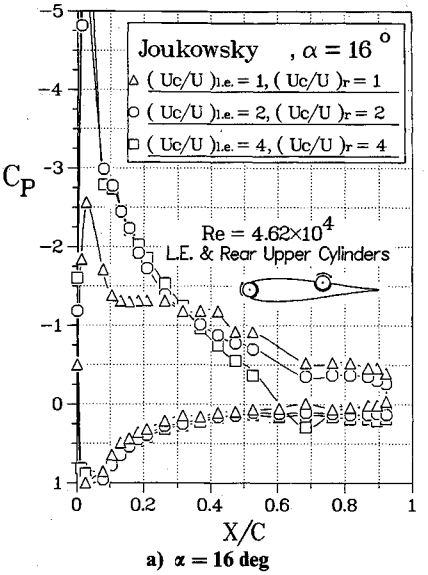

a) $\alpha = 16$ deg

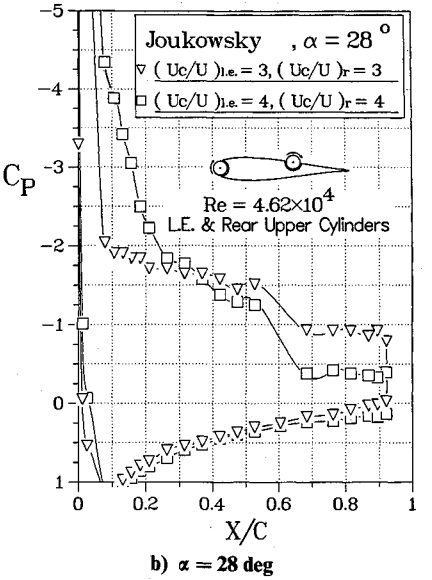

b) $\alpha = 28$ deg

Fig. 8 Typical pressure distribution plots with both leading-edge and rear upper-surface cylinders in operation.

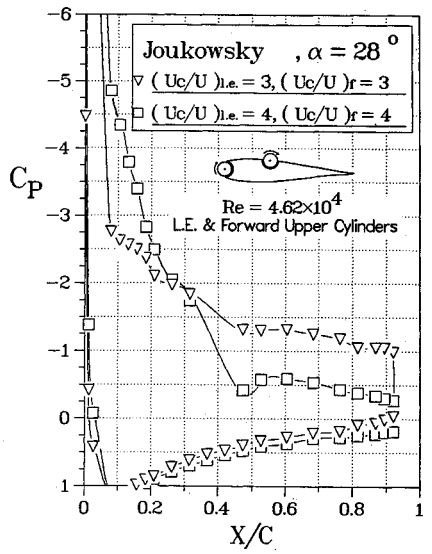

Fig. 9 Typical pressure distribution results with leading-edge and forward upper-surface cylinders, $\alpha = 28$ deg.

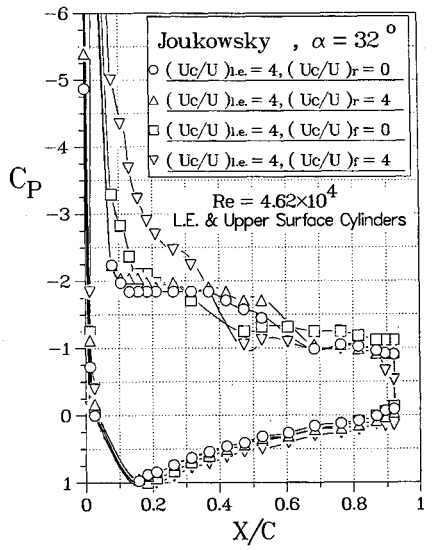

Fig. 10 Pressure plots as affected by combinations of the leading-edge and rear upper-surface cylinders' rotation.

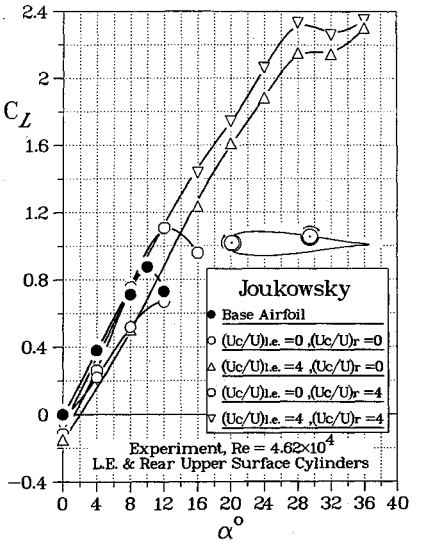

a) Rear upper-surface cylinder

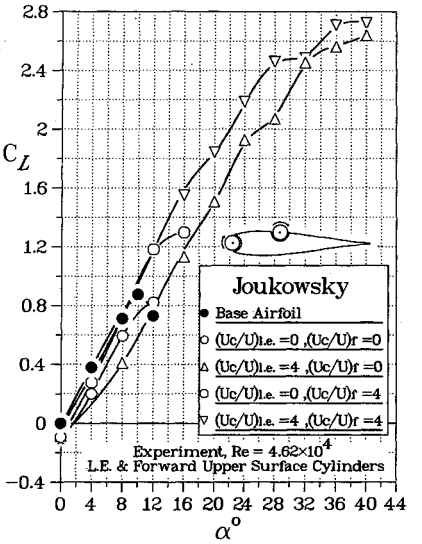

b) Forward upper-surface cylinder

Fig. 11 Lift and stall characteristics of the Joukowsky model with the leading-edge and upper-surface cylinders.

$U_c/U = 2$ prevents the initial separation of the flow behind the leading edge, and the flow remains attached over a substantial portion of the top surface. Finally, with the highest rate of rotation, there is a further recovery of the pressure with a significantly higher base value.

At $\alpha = 28$ deg, the flow was found to be separated over most of the airfoil even with the cylinders rotating at $U_c/U = 2$ (not shown). However, the size of the separated region decreases significantly with a further increase in the speed, particularly at $U_c/U = 4$. For $\alpha > 28$ deg, it was not possible to increase the size of the attached flow region by a further increase in U_c/U.

Similar general trends were observed for the forward upper-surface cylinder at $\alpha = 28$ deg, as shown in Fig. 9. The two cylinders in this configuration are closer together. Although their combined contributions show a larger pressure recovery near the trailing edge compared to the rear cylinder case (Fig. 8b), the size of the separated region is also increased.

Figure 10 attempts to summarize salient effects of the leading-edge and upper-surface cylinder rotations at a relatively high angle of attack of $\alpha = 32$ deg. The rotation of the leading-edge cylinder alone gives attached flow at the leading edge only, leaving the flow separated over most of the airfoil. Adding rotation of the rear upper-surface cylinder does not change the situation substantially. Only the combined effects of both the leading-edge and forward upper-surface cylinders decrease the adverse pressure gradient enough for the flow to remain attached up to around $X/C \approx 0.5$. The flow then separates in the form of a bubble with reattachment close to the trailing edge.

Influence of the leading-edge cylinder operating in conjunction with the forward or rear upper-surface cylinder can be better appreciated through the lift plots presented in Fig. 11. Performance of the original base airfoil (with sharp trailing edge and nose insert) as well as effect of its modifications through introduction of the cylinders are indicated to assess beneficial contribution of the cylinder rotation.

At the outset it is apparent that the change in geometry of the base airfoil and the presence of a gap affect both the $C_{L,\max}$ as well as the stall angle. However, as can be expected in light of the leading-edge cylinder data presented earlier in Fig. 5, $(U_c/U)_{le} = 1$ with $(U_c/U)_r = 1$ or $(U_c/U)_f = 1$ more than compensated for this initial loss giving $C_{L,\max}$ of around 1.2 and 1.3, respectively. Note that the upper-surface cylinders, rear or forward, while operating individually, are also able to make up for the loss (introduced by the airfoil modification), but they must rotate at a much higher speed. With both the leading-edge and rear upper-surface

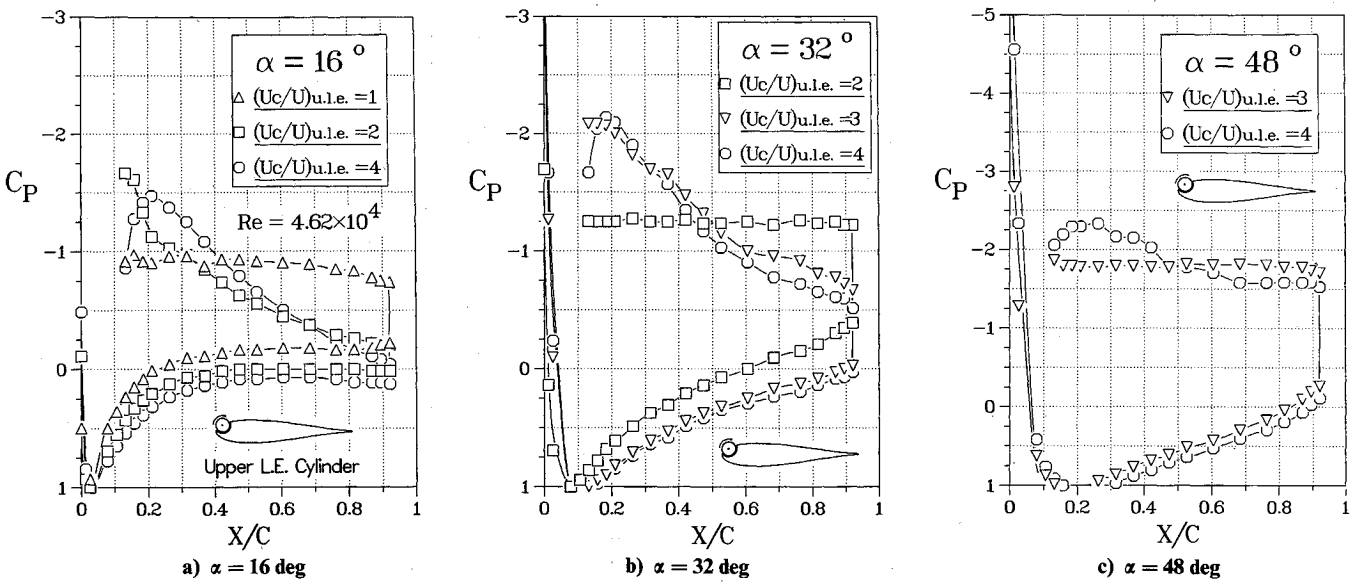

Fig. 12 Pressure distribution plots with the upper leading-edge cylinder.

cylinder rotating at $U_c/U = 4$, the stall is delayed to 28 deg with a $C_{L,\max}$ of around 2.35, an increase of 167% over the base airfoil data (Fig. 11a). Rotation of the forward upper-surface cylinder appears to be relatively more effective. With $(U_c/U)_{le} = (U_c/U)_f = 4$, additional improvement in performance is apparent with the stall angle now around 40 deg and a corresponding $C_{L,\max}$ of 2.73, an increase of approximately 210% (Fig. 11b). The pressure recovery results observed earlier in Fig. 9 also suggest favorable drag characteristics.

To summarize, a rotating leading-edge cylinder results in a large suction peak at the nose. However, depending on the angle of attack, the adverse pressure gradient still causes the flow to separate downstream. The use of a second cylinder on the upper surface helps to reduce the separated region. As far as the location of the upper surface cylinder is concerned, it is likely to be more effective in the front where the adverse pressure gradient is quite significant.

Effectiveness of the combination of leading-edge and forward upper-surface cylinders suggested a possibility of replacing the two by a single cylinder. This avoids the practical complications associated with construction, installation, and operation of two rotating cylinders.

The configuration, with a cylinder located at approximately 5% of the chord, was tested at cylinder speeds in the range of U_c/U up to 4. The results showed attached flow for angles of attack of as high as 48 deg. Several typical pressure plots as affected by the angle of attack and cylinder rotation are presented in Fig. 12.

At $\alpha = 16$ deg, all but the lowest speed of the cylinder rotation keep the flow attached over the top surface. As the rate of rotation is increased, the suction over the upper surface is generally increased except immediately behind the cylinder where a dip in the pressure profile becomes apparent at $U_c/U > 3$. This is due to the fact that the surface of the cylinder is higher than that of the airfoil, and the rotating cylinder is transferring momentum to the airfoil surface in this region. The discontinuity in the pressure plots near the leading edge is again due to difficulty in locating pressure taps close to and on the surface of the cylinder. Although the missing data are important for accurate calculation of the lift coefficient, this does not obscure the effects of cylinder rotation discussed presently.

At $\alpha = 32$ deg, the airfoil has stalled even with $U_c/U = 2$. Only the higher speeds of the cylinder ($U_c/U \geq 3$) are capable of keeping the upper-surface flow attached.

Finally, even at a very high incidence of $\alpha = 48$ deg, it is remarkable that the cylinder rotation at $U_c/U = 4$ is able to maintain partially attached flow over the upper surface. There

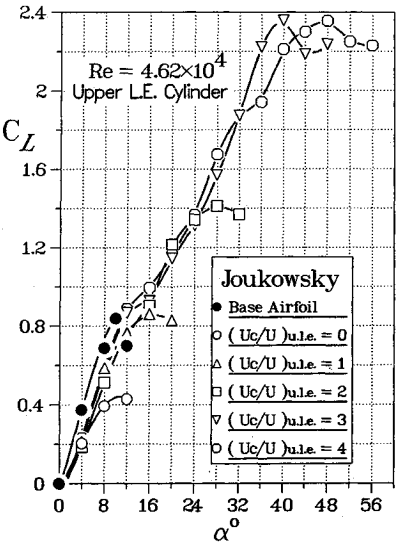

Fig. 13 Lift and stall characteristics of the Joukowsky model as affected by the upper leading-edge cylinder rotation. Base airfoil ($U_c/U = 0$) data serve as reference to assess the effect of airfoil modification by the cylinder and its rotation.

is, as can be expected, however, an associated drag penalty as is evident by the lack of any significant pressure recovery near the trailing edge.

The pressure profiles were integrated to yield the coefficients of lift plotted in Fig. 13. These values, however, are likely to be underestimated due to a lack of high-suction data over the rotating cylinder. In the absence of measured information, the pressure was conservatively approximated to remain locally constant, over the region with missing pressure taps, at the minimum observed value.

Compared to the leading-edge cylinder study (Fig. 5), where for $U_c/U = 4$, $C_{L,\max} \approx 2$ and $\alpha_{stall} \approx 28$ deg, now we have $C_{L,\max} \approx 2.35$ with $\alpha_{stall} \approx 48$ deg. This clearly suggests that location of the cylinder near the leading edge can significantly affect the airfoil performance. Thus, there is room for a systematic study to arrive at an optimum location.

Even compared to the results obtained using the leading-edge cylinder together with the forward upper-surface cylinder, performance of the present single cylinder configuration appears attractive. Although the $C_{L,\max}$ is slightly lower (down from 2.73 to 2.35), the stall is delayed from around 40–48 deg.

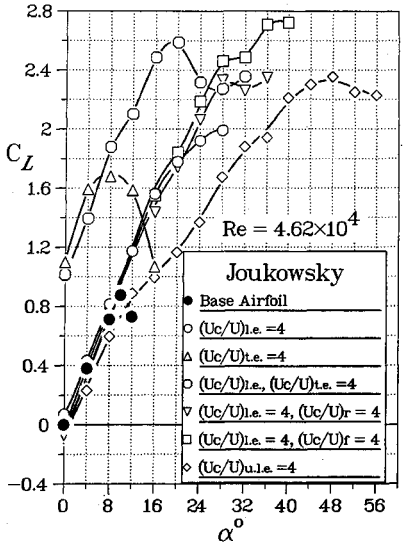

Fig. 14 Plots to assess relative influence of different configurations studied on the lift and stall characteristics.

However, the main advantage would be the mechanical simplicity of working with one cylinder.

With a vast amount of data obtained through a planned experimental program using the configurations presented earlier, it would now be useful to compare their distinctive features to help establish relative merits. Figure 14 attempts to achieve this objective. Trailing-edge cylinder results[14] are also included to permit more comprehensive comparison. Results of the standard Joukowsky airfoil (symmetrical, 15% thickness), with its $C_{L,\max} = 0.88$ and $\alpha_{\text{stall}} = 10$ deg, serve as reference for all the cases presented.

The leading-edge cylinder is quite effective in extending the lift curve, without significantly changing its slope, thus substantially increasing the maximum lift coefficient (1.75) and delaying the stall angle (28 deg). Further improvements in the maximum lift coefficient and stall angle are possible when the leading-edge cylinder is used in conjunction with an upper-surface cylinder. This configuration also results in a lower drag due to a large recovery of pressure near the trailing edge, at moderately high angles of attack. The $C_{L,\max}$ realized with the leading-edge and forward upper-surface cylinders, was about 2.73 ($\alpha = 36$ deg), approximately three times that of the base configuration.

A rotating cylinder on the upper side of the leading edge also proves very effective. Although the maximum coefficient of lift realized with its rotation is slightly lower (≈ 2.35), it does have a major advantage in terms of mechanical simplicity. Note, now the lift curve has a lower slope and is not an extension of the base airfoil lift curve. Hence, the lift at a given α is relatively lower; however, the stall is delayed to around 48 deg.

On the other hand, to improve lift over the range of low to medium angles of attack ($\alpha \leq 20$ deg), the trailing-edge cylinder proves much more effective,[14] particularly in conjunction with the leading-edge cylinder. The suction over the airfoil upper surface as well as the compression on the lower surface are increased dramatically with the higher rates of rotation of this cylinder, resulting in a substantial increase in lift ($\approx 195\%$).

Thus, depending on the intended objective in terms of desired $C_{L,\max}$ and stall angle, one can select an appropriate configuration to initiate a preliminary design.

Flow Visualization Study

The flow visualization study was carried out in a closed-circuit water channel facility. The model was constructed from Plexiglas and fitted with a leading-edge cylinder, driven

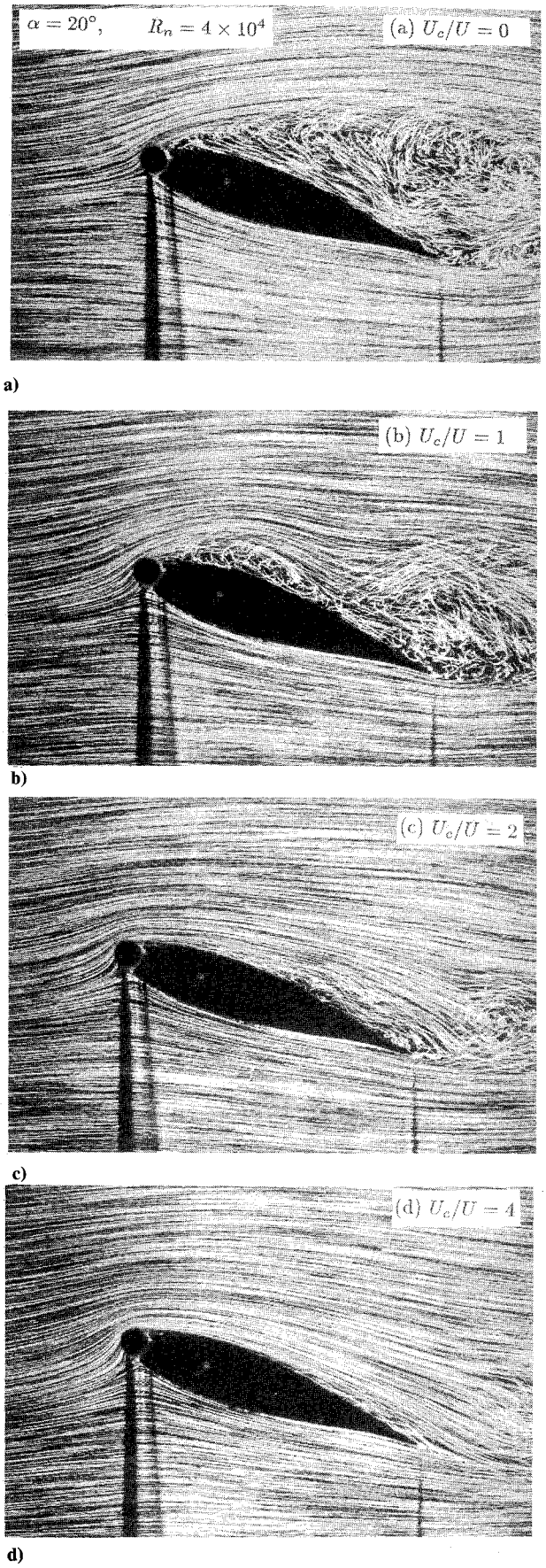

Fig. 15 Typical flow visualization photographs showing a remarkable effectiveness of the moving surface boundary-layer control method: a) highly separated flow, at a high angle of attack, in absence of the cylinder rotation; b) appearance of a separation bubble, $U_c/U = 1$; c) downward shift of the separation point with a distinct reduction in the wake width, $U_c/U = 2$; d) essentially attached flow, $U_c/U = 4$.

by a compressed-air motor. A suspension of fine polyvinyl chloride powder was used in conjunction with slit lighting to visualize streaklines. Both angle of attack and cylinder speeds were systematically changed and still photographs as well as a video movie were taken.

The study showed, rather dramatically, the effectiveness of this form of boundary-layer control (Fig. 15). With the model at $\alpha = 20$ deg and in absence of the cylinder rotation, a well-defined early separation resulting in a wide wake is quite apparent, with large-scale vortices sweeping away downstream. However, with the cylinder rotating at $U_c/U = 4$, an essentially attached flow is established over most of the upper surface of the airfoil.

At relatively lower rates of cylinder rotation, the flow character was found to be similar to that observed at $U_c/U = 1$, with the separation and reattachment regions progressively shifting downstream as the rotation rate increased. This is apparent through a progressive increase in U_c/U from 0 to 4.

In fact, the flow pattern was found to be quite unsteady with the vortex layer separating and forming a bubble on reattachment, the whole structure drifting downstream, diffusing, and regrouping at different scales of vortices. Ultimately the flow sheds large as well as small vortices. This unsteady character of the separating shear layer and the wake is clearly evident in the video, which was shown at the 27th Aerospace Sciences Meeting. Thus, the flow character suggested by the experimentally obtained time-average pressure plots appears to be a fair description of the process. Furthermore, this also suggests that analytical or numerical modeling of such highly complex and transient flow would pose a challenging problem.

Conclusions

The experimental investigation with a symmetrical Joukowsky airfoil using leading-edge and upper-surface rotating cylinders brings to light several interesting points of information:

1) In general, rotation of the leading-edge cylinder results in increased suction over the nose. It is the propagation of this lower pressure downstream, however, that determines the effectiveness of the rotation. This depends mainly on the geometry of the nose and smoothness of transition from the cylinder of the airfoil surface. A large gap (>3 mm) substantially decreases beneficial effect of the cylinder rotation.

2) The increased momentum injection into the boundary layer, with an increase in speed of rotation, delays the separation of flow from the upper surface (stall), resulting in a higher $C_{L,\max}$. The existence of a critical speed is also evident beyond which momentum injection through a moving surface appears to have relatively less effect.

3) With the rotation of the leading-edge cylinder, the onset of flow separation occurs at relatively higher angles of attack. The upper surface flow remains attached up to a distance downstream of the leading edge, at which point it separates, leading to a large separation bubble, with reattachment toward the trailing edge. The flow, therefore, is not completely separated from the airfoil, thus resulting in a flatter stall peak.

4) The use of a leading-edge cylinder extends the lift curve without substantially changing its slope, thus considerably increasing the maximum lift coefficient and stall angle. The Joukowsky model showed an increase in $C_{L,\max}$ by around 125%, with the stall delayed from 10 to 28 deg.

5) In contrast to the leading-edge cylinder, the use of a trailing-edge cylinder substantially increases the lift before stall.[14] The rotating trailing-edge cylinder acts like a flap shifting the C_L vs α plots to the left. A high rate of rotation of this cylinder results in a dramatic increase in suction over the airfoil upper surface, thus giving a larger lift. Furthermore, it can be used in conjunction with the leading-edge cylinder, resulting in impressive values of lift over the whole range of low to moderately high angles of incidence ($\alpha \leq 18$ deg).

6) Presence of a steep positive pressure gradient near the leading edge of the airfoil at large angles of attack requires the rotation of the nose-cylinder to avoid separation at that point. But depending on the angle of attack, the adverse pressure gradient may still cause flow separation further downstream. Since the flow remains attached at the leading edge, the lift continues to increase with the angle of attack, whereas the flow remains separated over most of the upper surface, resulting in an increase in pressure drag (as evident from a reduced pressure recovery at the trailing edge). The use of a second cylinder is now required to further improve the lift and stall characteristics.

7) Protrusion of the upper-surface cylinders in the flow has an adverse effect on the aerodynamic characteristics of the airfoil at low angles of attack. In absence of the cylinder rotation, the flow separates at the location of the cylinder, resulting in a decrease in lift and an increase in drag. However, their rotation increases the $C_{L,\max}$ and delays stall. The forward upper-surface cylinder is particularly effective in this respect. This is, in fact, expected since the adverse pressure gradient is highest close to the leading edge. Further improvements in the $C_{L,\max}$ and stall angle are possible when the forward upper-surface cylinder is used in conjunction with the leading-edge cylinder. This configuration is expected to result in lower drag due to almost complete recovery of pressure at the trailing edge even at moderately high angles of attack. The increase in $C_{L,\max}$ was observed to be around 210%, with the stall delayed to 36 deg ($U_c/U = 4$ for both the cylinders).

8) The configuration with a rotating cylinder on the upper side of the leading edge appears to be quite promising. Although the peak $C_{L,\max}$ realized with the cylinder rotation was slightly less (2.35 against 2.73) compared to the two-cylinder configuration, it does have a major advantage in being mechanically simple in terms of design and application. The increase in $C_{L,\max}$ at $U_c/U = 4$ by around 167% and the delay in stall from 10 to 48 deg is quite impressive.

9) A reliable method for blockage correction at a high angle of attack, when the aerofoil behaves as a bluff body with an unsteady separation bubble and the wake, is badly needed. In absence of such a procedure, the results have been purposely presented without wall confinement corrections. The flow visualization pictures clearly show the effect of momentum injection at a given blockage.

Acknowledgments

The models were fabricated in the Mechanical Engineering workshop at the University of British Columbia. Assistance of Ed Abell, Senior Technician, in design and construction of the models is gratefully acknowledged. The research work was supported by the Natural Sciences and Engineering Council of Canada, Grant A-2181.

References

[1]Goldstein, S., *Modern Developments in Fluid Mechanics*, Vols. I and II, Oxford University, Oxford, England, 1938.

[2]Lachmann, G. V., *Boundary Layer and Flow Controls*, Vols. I and II, Pergamon, London, 1961.

[3]Rosenhead, L., *Laminar Boundary Layers*, Oxford University, Oxford, England, 1966.

[4]Schlichting, H., *Boundary Layer Theory*, McGraw-Hill, New York, 1968.

[5]Chang, P. K., *Separation of Flow*, Pergamon, New York, 1970.

[6]Modi, V. J., Sun, J. L. C., Akutsu, T., Lake, P., MacMillan, K., Swinton, P. J., and Mullins, D., "Moving Surface Boundary-Layer Control for Aircraft Operation at High Incidence," *Journal of Aircraft*, AIAA, Vol. 18, No. 11, 1981, pp. 963–968.

[7]Favre, A., "Contribution a l'Etude Experimentale des Mouvements Hydrodynamiques a Deux Dimensions," Thesis presented to the University of Paris, France, 1938.

[8]Alvarez-Calderon, A., and Arnold, F. R., "A Study of the Aerodynamic Characteristics of a High Lift Device Based on Rotating Cylinder Flap," Stanford Univ., Stanford, CA, Tech. Rept. RCF-1, 1961.

[9]Brown, D. A., "Peruvians Study Rotating-Cylinder Flap," *Aviation Week and Technology*, Vol. 88, No. 23, 1964, pp. 70–76.

[10]Cichy, D. R., Harris, J. W., and MacKay, J. K., "Flight Tests of a Rotating Cylinder Flap on a North American Rockwell YOV-10A Aircraft," NASA CR-2135, Nov. 1972.

[11]Weiberg, J. A., Giulianettij, D., Gambucci, B., and Innis, R. C., "Takeoff and Landing Performance and Noise Characteristics of a Deflected STOL Airplane with Interconnected Propellers and Rotating Cylinder Flaps," NASA TM X-62, 320, Dec. 1973.

[12]Cook, W. L., Hickey, D. H., and Quigley, H. C., "Aerodynamics of Jet Flap and Rotating Cylinder Flap STOL Concepts," AGARD Fluid Dynamics Panel on V/STOL Aerodynamics, Paper 10, Delft, The Netherlands, April 1974.

[13] Mokhtarian, F., and Modi, V. J., "Fluid Dynamics of Airfoils with Moving Surface Boundary Layer Control," AIAA Paper 86-2184, Aug. 1986; also *Journal of Aircraft*, Vol. 25, 1988, pp. 163–169.

[14]Mokhtarian, F., Modi, V. J., and Yokomizo, T., "Effect of Moving Surfaces on the Airfoil Boundary-Layer Control," AIAA Paper 88-4303, Aug. 1988; also *Journal of Aircraft*, Vol. 27, 1990, pp. 44–50.